ANTIOXIDANTS & REDOX SIGNALING
Volume 21, Number 4, 2014

DOI: 10.1089/ars.2013.5420

Discoveries

ORIGINAL RESEARCH COMMUNICATION

SIRT3 Deacetylates ATP Synthase F_1 Complex Proteins in Response to Nutrient- and Exercise-Induced Stress

Athanassios Vassilopoulos,[1,2,*] J. Daniel Pennington,[3,*] Thorkell Andresson,[4] David M. Rees,[3] Allen D. Bosley,[4] Ian M. Fearnley,[3] Amy Ham,[5] Charles Robb Flynn,[6] Salisha Hill,[7] Kristie Lindsey Rose,[7] Hyun-Seok Kim,[8] Chu-Xia Deng,[2] John E. Walker,[3] and David Gius[1]

Abstract

Aims: Adenosine triphosphate (ATP) synthase uses chemiosmotic energy across the inner mitochondrial membrane to convert adenosine diphosphate and orthophosphate into ATP, whereas genetic deletion of *Sirt3* decreases mitochondrial ATP levels. Here, we investigate the mechanistic connection between SIRT3 and energy homeostasis. ***Results:*** By using both *in vitro* and *in vivo* experiments, we demonstrate that ATP synthase F_1 proteins alpha, beta, gamma, and Oligomycin sensitivity-conferring protein (OSCP) contain SIRT3-specific reversible acetyl-lysines that are evolutionarily conserved and bind to SIRT3. OSCP was further investigated and lysine 139 is a nutrient-sensitive SIRT3-dependent deacetylation target. Site directed mutants demonstrate that $OSCP^{K139}$ directs, at least in part, mitochondrial ATP production and mice lacking *Sirt3* exhibit decreased ATP muscle levels, increased ATP synthase protein acetylation, and an exercise-induced stress-deficient phenotype. ***Innovation:*** This work connects the aging and nutrient response, *via* SIRT3 direction of the mitochondrial acetylome, to the regulation of mitochondrial energy homeostasis under nutrient-stress conditions by deacetylating ATP synthase proteins. ***Conclusion:*** Our data suggest that acetylome signaling contributes to mitochondrial energy homeostasis by SIRT3-mediated deacetylation of ATP synthase proteins. *Antioxid. Redox Signal*. 21, 551–564.

Introduction

AN INTRIGUING FINDING from our previous work (11) and that of others (1) demonstrated that cells lacking *Sirt3* exhibited altered mitochondrial metabolism, including a significant decrease in mitochondrial adenosine triphosphate (ATP) levels. Mitochondria are central to aging and age-related diseases such as insulin resistance, neurodegeneration, and carcinogenesis by tightly regulating the reactive oxygen species that are generated as a byproduct of normal respiration activities (25). Chemical reactions in a cell that are critical for the maintenance of cellular viability are thermodynamically dependent on the mitochondria to maintain a mass action ratio of ATP and adenosine diphosphate (ADP) for approximately ten orders of magnitude away from equilibrium. The ATP synthase (F_1F_o ATPase), an evolutionarily

[1]Department of Radiation Oncology, Robert H. Lurie Comprehensive Cancer Center, Feinberg School of Medicine, Northwestern University, Chicago, Illinois.
[2]Genetics of Development and Disease Branch, National Institute of Diabetes, Digestive and Kidney Diseases, National Institutes of Health, Bethesda, Maryland.
[3]Medical Research Council Mitochondrial Biology Unit, Wellcome Trust/Medical Research Council Building, Cambridge, United Kingdom.
[4]Laboratory of Proteomics and Analytical Technologies, Advanced Technology Program, SAIC-Frederick, Inc., Frederick National Laboratory for Cancer Research, Frederick, Maryland.
[5]Department of Pharmaceutical, Social and Administrative Science, College of Pharmacy, Belmont University, Nashville, Tennessee.
[6]Department of Surgery, Vanderbilt University School of Medicine, Nashville, Tennessee.
[7]Mass Spectrometry Research Center, Vanderbilt University School of Medicine, Nashville, Tennessee.
[8]Department of Life Science, College of Natural Science Ewha Womans University, Seoul, Korea.
*The first two authors contributed equally to this work.

Innovation

This work connects the aging and nutrient response, *via* SIRT3 direction of the mitochondrial acetylome, to the regulation of mitochondrial energy homeostasis under nutrient-stress conditions by deacetylating adenosine triphosphate (ATP) synthase proteins. In this study, using proteomic analysis of both *in vitro* and *in vivo* samples, multiple reversible acetyl-lysines were identified in the alpha, beta, gamma, and oligomycin sensitivity-conferring protein subunits of the ATP synthase complex proteins that are evolutionarily conserved. The results presented here suggest that in addition to its role in reactive oxygen species signaling by directing MnSOD activity, SIRT3 can regulate ATP levels by deacetylating the ATP synthase complex.

conserved protein complex, uses chemiosmotic energy that is stored in a gradient across the mitochondrial inner membrane to convert ADP and orthophosphate to ATP (29). There is a membrane-bound portion (F_o) and a central stalk (F_1) containing a catalytic domain, held by a peripheral stalk stator that extends into the matrix.

Rotational energy is generated by protons entering the F_o portion of the ATP synthase complex *via* a channel or channels between stationary subunit a and a rotary ring consisting of eight c subunits (29). The rotational movement is transmitted through a central stalk consisting of subunits γ, δ, and ε. The γ subunit of this asymmetrical stalk interacts with the nonrotating catalytic subunits consisting of 3 each of alternating α and β subunits. The spinning central stalk of the ATP synthase is held in place by an external stalk consisting of oligomycin sensitivity-conferring protein (OSCP), b, F6, and d subunits; OSCP sits at the top of the ATP synthase complex and appears to hold the α and β proteins in specific three-dimensional complexes (20). This stator is flexible, a trait that may have a role in maintaining contact with the rotating portion of the F_1 complex during ATP synthesis as well as in regulating enzymatic function (20).

Lysine acetylation is a reversible and highly regulated post-translational modification that is found in multiple nonhistone proteins (7). Acetylation takes place on lysine residues, neutralizing the positive charges on proteins, subsequently altering the three-dimensional structure as well as changing enzymatic function (14, 19). This process regulates diverse protein properties, including DNA–protein interactions, subcellular localization, transcriptional activity, protein stability, protein–protein interactions, and last, but not least, enzymatic activity (14, 19). Previously, a proteomic survey in mouse liver mitochondria revealed that a large number of mitochondrial proteins are subject to reversible lysine acetylation (13), establishing lysine acetylation as an abundant post-translational modification in the mitochondrion (3, 13). More recent proteomic analyses of lysine-acetylated mitochondrial proteins confirmed this and showed that acetylated proteins are involved in the tricarboxylic acid cycle, oxidative phosphorylation, β-oxidation of lipids, amino-acid metabolism, carbohydrate metabolism, nucleotide metabolism, and the urea cycle (3, 22, 24).

Based on these results, it seems reasonable to suggest that acetylation of mitochondrial proteins may play a role in maintaining and regulating mitochondrial metabolism and function. SIRT3 is the primary mitochondrial deacetylase (16), and genetic knockout of *Sirt3* results in decreased cellular ATP levels *in vitro* and *in vivo* (1). Thus, we believe it is a logical extension to hypothesize that SIRT3 functions as a mitochondrial regulatory protein, maintaining mitochondrial energy homeostasis *via* changes in the acetylation status of mitochondrial metabolic proteins, including perhaps those which comprise the ATP synthase complex. This idea would mechanistically connect a metabolic sensing/signaling protein, such as SIRT3, to the direct regulation of ATP synthase. Thus, it seems reasonable to propose that the ATP synthase complex would be a downstream target of SIRT3 in the regulation of energy generation.

Results

SIRT3 deacetylates multiple proteins in the ATP synthase complex

We (12) and others (1) demonstrated that cells lacking *Sirt3* exhibit a significant decrease in mitochondrial ATP levels and ATP synthase is a critical enzymatic complex which generates ATP in the mitochondria (28). Thus, it seemed reasonable to propose that SIRT3 may target proteins in the ATP synthase complex as a means of direct regulation of ATP synthase activity. To address this hypothesis, affinity-purified bovine mitochondrial ATP synthase was obtained using a Glutathione S-transferase-tagged inhibitor protein ($I_{1\text{-}60}$), and two 50 μg samples were resolved by sodium dodecyl sulfate polyacrylamide gel electrophoresis (SDS-PAGE) followed by either immunoblotting with a pan anti-acetyl-lysine antibody (Fig. 1a, lane 1) or staining with Coomassie (lane 2). These results demonstrate that multiple ATP synthase proteins are acetylated *in vivo*. These samples were subsequently treated with PCAF, which is an acetyl transferase previously shown to acetylate lysine residues, separated, and immunoblotted with an anti-acetyl antibody (Cell Signaling, Inc.) (lane 3 *vs.* 4). The PCAF-treated ATP synthase samples from lane 4 were subsequently mixed with recombinant SIRT3 without (lane 5) and with nicotinamide adenine dinucleotide (NAD) (lane 6) for a cell-free deacetylation assay (lane 5 *vs.* 6). Finally, the samples in Figure 1a, lanes 5 and 6 were isolated and analyzed by mass spectrometry, and these results identified 11 alpha, 6 beta, 3 gamma, and 1 OSCP *in vitro* reversible acetyl-lysines (Table 1).

In addition, to identify the presence of *in vivo* acetylation sites, liver mitochondria were isolated from both *Sirt3* wild-type (WT) and knockout mice that were initially tested for protein acetylation levels using a pan anti-acetyl antibody (Supplementary Fig. S1A; Supplementary Data are available online at www.liebertpub.com/ars). After detecting increased acetylation in the $Sirt3^{-/-}$ mice, samples were in-solution tryptic digested followed by purification of acetylated peptides with immunoprecipitation using an agarose bead-conjugated anti-acetyl lysine antibody. Finally, the enriched acetylated peptides were analyzed by mass spectrometry. Consistent with the *in vitro* results, multiple peptides corresponding to different ATP synthase subunits were found to be acetylated *in vivo* in liver mitochondria from *Sirt3*-deficient mice compared with WT mice (Table 2). These results suggest that the ATP synthase complex, which is critical to the generation of mitochondrial ATP, contains multiple SIRT3 deacetylation targets.

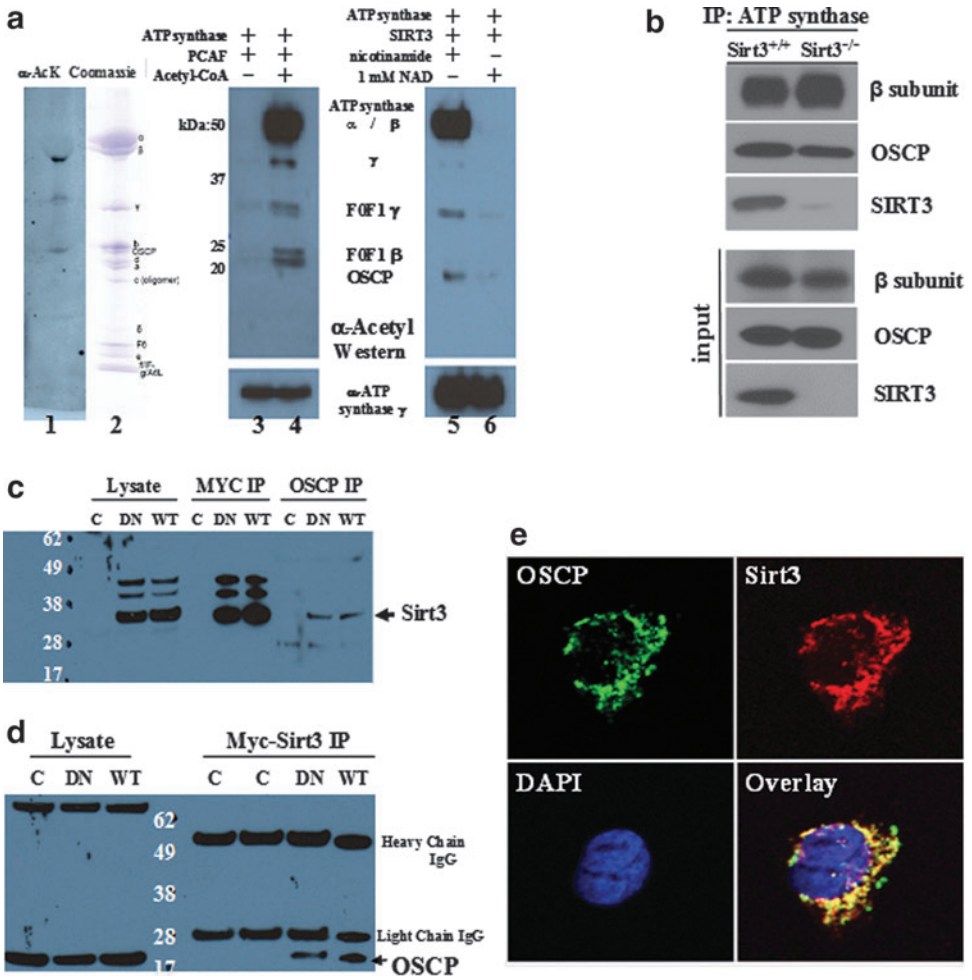

FIG. 1. The adenosine diphosphate (ATP) synthase complex contains multiple proteins with reversible acetyl-lysines and interacts with SIRT3. (a) Left panel, two 50 μg samples of highly purified bovine F1Fo ATP synthase were separated, transferred, and blotted with an acetyl-lysine antibody (Cell Signaling, Inc.) or stained with Coomassie. Middle panel, purified bovine F1Fo ATP synthase was treated with PCAF and blotted. Right panel, purified bovine F1Fo ATP synthase treated with PCAF was purified, treated with recombinant human SIRT3, and blotted with an acetyl-lysine antibody. **(b)** Skeletal muscle mitochondrial lysates from $Sirt3^{+/+}$ and $Sirt3^{-/-}$ mice were harvested, IPed with an anti-ATP synthase antibody (Abcam, Inc.), and subsequently immunoblotted with an anti-OSCP antibody (Santa Cruz Biotechnology, Inc.), anti-ATP synthase β subunit (Abcam, Inc.), or anti-SIRT3 antibody (Cell Signaling, Inc.). **(c-d)** SIRT3 physically interacts with oligomycin sensitivity-conferring protein (OSCP). HCT116 cells were constructed to constitutively express a Myc-tagged *SIRT3* gene, and cell extracts were **(c)** IPed with either an anti-Myc or an OCSP antibody and immunoblotted with an anti-SIRT3 antibody, or **(d)** IPed with an anti-Myc antibody and immunoblotted with an OCSP antibody. **(e)** IHC staining with an anti-SIRT3 and anti-OSCP antibody, with the images merged in the lower right section. Representative micrographs are shown.

ATP synthase complex proteins physically interact with SIRT3

In order to connect SIRT3 to the ATP synthase complex, experiments were performed to identify a direct enzyme-substrate interaction. As such, mitochondrial lysates from both $Sirt3^{+/+}$ and $Sirt3^{-/-}$ mice were harvested, immunoprecipitated (IPed) with an anti-ATP synthase antibody (Abcam, Inc.), separated into two equal fractions, and, subsequently, immunoblotted with an anti-ATP synthase β subunit, anti-OSCP (Abcam, Inc.), or anti-SIRT3 antibody (Cell Signaling, Inc.). These results clearly show that SIRT3 interacts with the ATP synthase complex, implying that one or more ATP synthase proteins may be legitimate SIRT3 deacetylation targets (Fig. 1b). It has been previously shown that SIRT1 can regulate transcription of MnSOD, a SIRT3-specific deacetylase substrate (18), suggesting that it is possible that there are redundant pathways between SIRT1 and SIRT3 for regulating mitochondrial proteins. However, after subcellular fractionation, we could not detect any SIRT1 in the mitochondria (Supplementary Fig. S1B), indicating that SIRT1 cannot co-localize with OSCP and ATP synthase *in vivo*. Moreover, in contrast to the observed interaction of ATP synthase with SIRT3, we could not detect an interaction with SIRT1 (Supplementary Fig. S1C), which excludes the possibility that SIRT1 can regulate ATP synthase by directly affecting post-translational acetylation. To address the idea that SIRT3 deacetylates one or more proteins within the ATP

Table 1. *In Vitro* SIRT3 Deacetylation Targets

Amino acid	Sequence	Spectral Count Pre	Spectral Count Post
ATP synthase subunit alpha			
132	LIKEGDVVKR	4	1
161	VVDALGNAIDGKGPI	5	0
167	LGNAIDGKGPIGSKT	3	1
230	TSIAIDTIINQKR	5	1
239	FNDGTDEKK	2	0
240	FNDGTDEKKK	3	1
261	RSTVAQLVKR	6	2
427	AMKQVAGTMK	12	4
434	VAGTMKLELAQYR	4	1
531	SDGKISEQSDAKLK	7	2
539	ISEQSDAKLK	4	1
ATP synthase subunit beta			
55	AAQASPSPKAGATT	2	0
124	GQKVLDSGAPIRIPV	5	1
197	VVDLLAPYAKGGK	2	0
259	MIESGVINLKDATSK	2	0
426	GVQKILQDYK	4	0
522	KADKLAEEHS	3	1
ATP synthase subunit gamma			
89	ADIKAPEDKKK	6	0
138	IKGILYR	4	0
154	THSDQFLVSFKDVGR	3	1
ATP synthase subunit OSCP			
139	TVLKSFLSPNQILK	6	1
ATP synthase subunit MnSOD			
68	NVTEEKYQEALAK	5	0
122	GELLEAKRDFGS	4	1

In vitro deacetylation assays from cell extracts treated with SIRT3 and sent for mass spectrometry.
Pre, before SIRT3 addition; Post, after SIRT3 addition.

synthase complex, additional experiments focusing on the OSCP ATP synthase complex protein were performed, as OSCP appeared to have only one reversible acetyl-lysine based on our mass spectrometry data and it has been previously considered to play a role in the regulation of ATP synthase activity (21, 28).

Therefore, OSCP was IPed from HCT116 cells genetically altered to overexpress the WT *Myc-SIRT3* gene (HCT116-Sirt3-wt) as previously described (9) and a control cell line that lacked overexpression. These samples were subsequently resolved by PAGE, immunoblotted with an anti-SIRT3 antibody, and showed an OSCP interaction with the SIRT3 WT and deacetylation null (DN) mutant (Fig. 1c). A myc-IPed SIRT3 immunoblot was also done as an internal control. In addition, a MYC-IP and anti-OSCP immunoblot confirmed the interaction between these two proteins (Fig. 1d). Finally, HCT116 cells constitutively expressing WT SIRT3 were stained by immunohistochemistry with antibodies to OSCP and SIRT3 (Fig. 1e) or OSCP, SIRT3, and mitotracker (Supplementary Fig. S1B), and these results confirmed that OSCP and SIRT3 co-localize to the mitochondria.

Table 2. SIRT3 Targets in Wild-Type *Versus* *Sirt3*$^{-/-}$ Liver

Subunits	Ac-peptides count *Sirt3*$^{-/-}$	Ac-peptides count *Sirt3*$^{+/+}$
ATP synthase alpha	132	162
ATP synthase beta	87	75
ATP synthase gamma	67	61
ATP synthase delta	21	22
ATP synthase b	189	161
ATP synthase d	368	298
ATP synthase e	10	10
ATP synthase f	4	4
ATP synthase g	14	8
ATP synthase O (OSCP)	232	152

Acetylated peptides found in wild-type and knockout liver extracts after mass spectrometry.

OSCP contains a reversible acetyl-lysine that is deacetylated by SIRT3 and restores ATP levels

To determine whether SIRT3 was capable of deacetylating specific subunits of the ATP synthase, an *in vitro* deacetylation assay using human recombinant SIRT3 (BioMol, Inc.) and purified bovine OSCP was performed (Fig. 2a). Reaction products were separated by SDS-PAGE and detected with an anti-acetyl antibody showing that the OSCP subunit of the ATP synthase is significantly deacetylated by SIRT3 (lane 1 *vs.* 2) compared with other subunits. Consistent with this result, the decrease in lysine acetylation was inhibited by either addition of nicotinamide (lane 3), an inhibitor of sirtuin reactions, or removal of NAD+ (lane 4), suggesting that deacetylation is directly due to SIRT3 activity.

Further evidence that OSCP contains reversible acetyl-lysine residues was obtained when WT mice were fasted for 36 h, and their livers were harvested and solubilized. These samples were subsequently divided into equal fractions, resolved by SDS-PAGE, and immunoblotted with either a pan anti-acetyl (Fig. 2b, upper panel) or an anti-OSCP antibody (Fig. 2b, lower panel), showing that OSCP acetylation was decreased in the livers from fasting mice. In addition, total mitochondrial protein lysine acetylation was also shown to be increased in the *Sirt3*$^{-/-}$ mice under normal conditions as well as after fasting (Supplementary Fig. S2B). Finally, ATP levels in the *Sirt3*$^{-/-}$ mouse embryonic fibroblasts (MEFs) were significantly less than observed in the *Sirt3*$^{+/+}$ MEFs (Fig. 2c), as has been shown by others (1, 11).

To determine whether SIRT3 directly deacetylates OSCP, two lentiviruses that express either the WT (lenti-Sirt3-wt) or a DN mutant (lenti-Sirt3-dn) *Sirt3* gene (a gift from Dr. Toren Finkel, NHLBI, NIH) in which amino acid 248 was changed from a histidine to tyrosine (1) were used. *Sirt3*$^{-/-}$ MEFs were infected with these two viruses and a control lentivirus, IPed with an anti-OSCP antibody, divided into equal fractions, resolved by SDS-PAGE, and immunoblotted with either an anti-acetyl (Fig. 2d, upper panel) or an anti-OSCP antibody (Fig. 2d, middle panel). Equal levels of exogenously expressed *Sirt3* were confirmed by immunoblotting with an anti-myc antibody (lower panel), as both the WT and the DN *Sirt3* genes contained a myc tag sequence. These experiments demonstrated that WT, but not DN *Sirt3*, decreases OSCP acetylation (Fig. 2d, upper panel, lane 3 *vs.* 2). Finally, the observed decreased acetylation was associated with increased mitochondrial ATP levels in *Sirt3*$^{-/-}$ MEFs (Fig. 2e), though not quite to the levels observed in *Sirt3*$^{+/+}$ MEFs

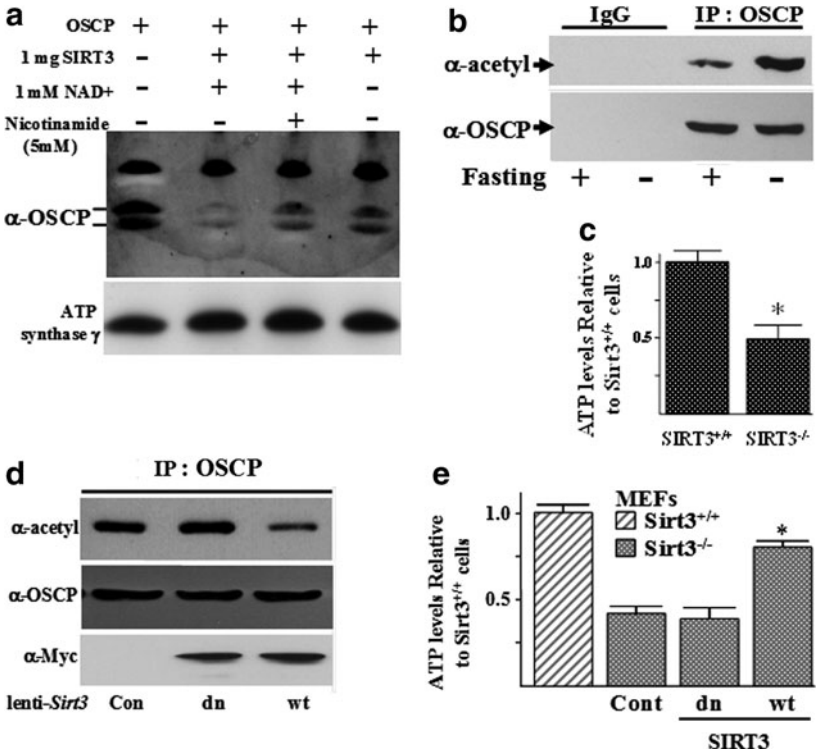

FIG. 2. ***Sirt3*** **knockout cells have increased mitochondrial acetylated protein and decreased ATP levels, and OSCP contains a reversible acetyl-lysine.** **(a)** Bovine purified OSCP was mixed with or without recombinant SIRT3 in the presence or absence of nicotinamide and/or NAD+. After 1 h, samples were separated by PAGE, followed by immunoblotting with an anti-acetyl antibody (Cell Signaling, Inc.). Antibody against ATP synthase subunit γ was used as a loading control. **(b)** OSCP contains a reversible acetyl-lysine. Livers from isogenic, 3-month-old $Sirt3^{+/+}$ mice on an AL diet (−) or fasted for 36 h (+) were harvested, IPed with an anti-OSCP antibody, and immunoblotted with an anti-acetyl antibody or anti-OSCP antibody. **(c)** Mitochondrial ATP levels in Sirt3 wild-type and knockout cells. $Sirt3^{+/+}$ and $Sirt3^{-/-}$ MEFs were lysed, and ATP levels were measured using a chemiluminescence assay. Data are presented as arbitrary luminescence units for ATP levels as a ratio (or compared with) of the level in $Sirt3^{+/+}$ MEFs. **(d, e)** Re-expression of wild-type, but not a deacetylation null mutant of *Sirt3*, **(d)** deacetylates OSCP and **(e)** restores ATP levels in $Sirt3^{-/-}$ MEFs. Fifth-passage $Sirt3^{-/-}$ MEFs were transfected with a control lentivirus (Cont), virus expressing a wild-type Sirt3 (wt), or one expressing the deacetylation null gene (dn) in which amino acid 248 has been changed from a histidine to tyrosine (1). Forty hours after infection, $Sirt3^{-/-}$ MEFs were harvested and mitochondrial extracts were IPed with an anti-OSCP antibody followed by immunoblotting with an anti-acetyl or anti-OSCP antibody. These extracts were also used to measure ATP levels as described earlier in **(b)**. ATP levels are presented as a ratio compared with the levels observed in $Sirt3^{+/+}$ MEFs. The results of all the experiments in this figure were obtained from at least three independent replicates. Representative gels are shown. Error bars represent one standard deviation. *Indicates $p < 0.05$ by *t*-test.

(hatched bar). These results support the hypothesis that SIRT3 directly deacetylates OSCP and that a change in the acetylation status of at least one ATP synthase complex protein results in an increase in ATP levels.

SIRT3 deacetylates lysine 139 of OSCP

To detect specific lysines that might be direct deacetylation targets for SIRT3, total mouse liver mitochondrial proteins from $Sirt3^{+/+}$ and $Sirt3^{-/-}$ mice were resolved by SDS-PAGE. Bands were excised and individually digested with trypsin before analysis by mass spectrometry in an OrbiTrap mass spectrometer. OSCP was identified in both samples, as expected, but peptides modified by acetylation of lysine 139 were only detected in the $Sirt3^{-/-}$ samples. Of the 13 most intense peaks in this tandem mass spectrum, 8 are attributable to OSCP fragments. Six peaks correspond to a series of y+ type fragment ions defining a partial amino-acid sequence of K(Ac)SFLS. One peak is a b+ type ion, b2, and an additional peak of high intensity corresponds to the 126.0913 m/z immonium ion produced by the fragmentation of peptides containing ε-acetylated lysine and is diagnostic of this modification. The lysine in the K(Ac)SFLS sequence is located at OSCP amino acid position 139 of the mitochondrial cleaved protein (163 for the full-length protein). A representation of the tandem mass spectrum demonstrating the acetylation of lysine 139 in a tryptic peptide is shown (Fig. 3a). In addition, livers from $Sirt3^{+/+}$ and $Sirt3^{-/-}$ mice were harvested, and tandem mass spectrometry showed a significant increase in the acetylation of OSCP lysine 139 in the $Sirt3^{-/-}$ as compared with the $Sirt3^{+/+}$ mice (Fig. 3b).

The specificity of this lysine deacetylation was determined using recombinant human SIRT3 and a synthetic peptide (JPT Peptide Technologies) corresponding to a 20-amino-acid OSCP sequence containing lysine 139. This peptide (sequence EEATLSELKTVL(AcK)SFLSQGQ)

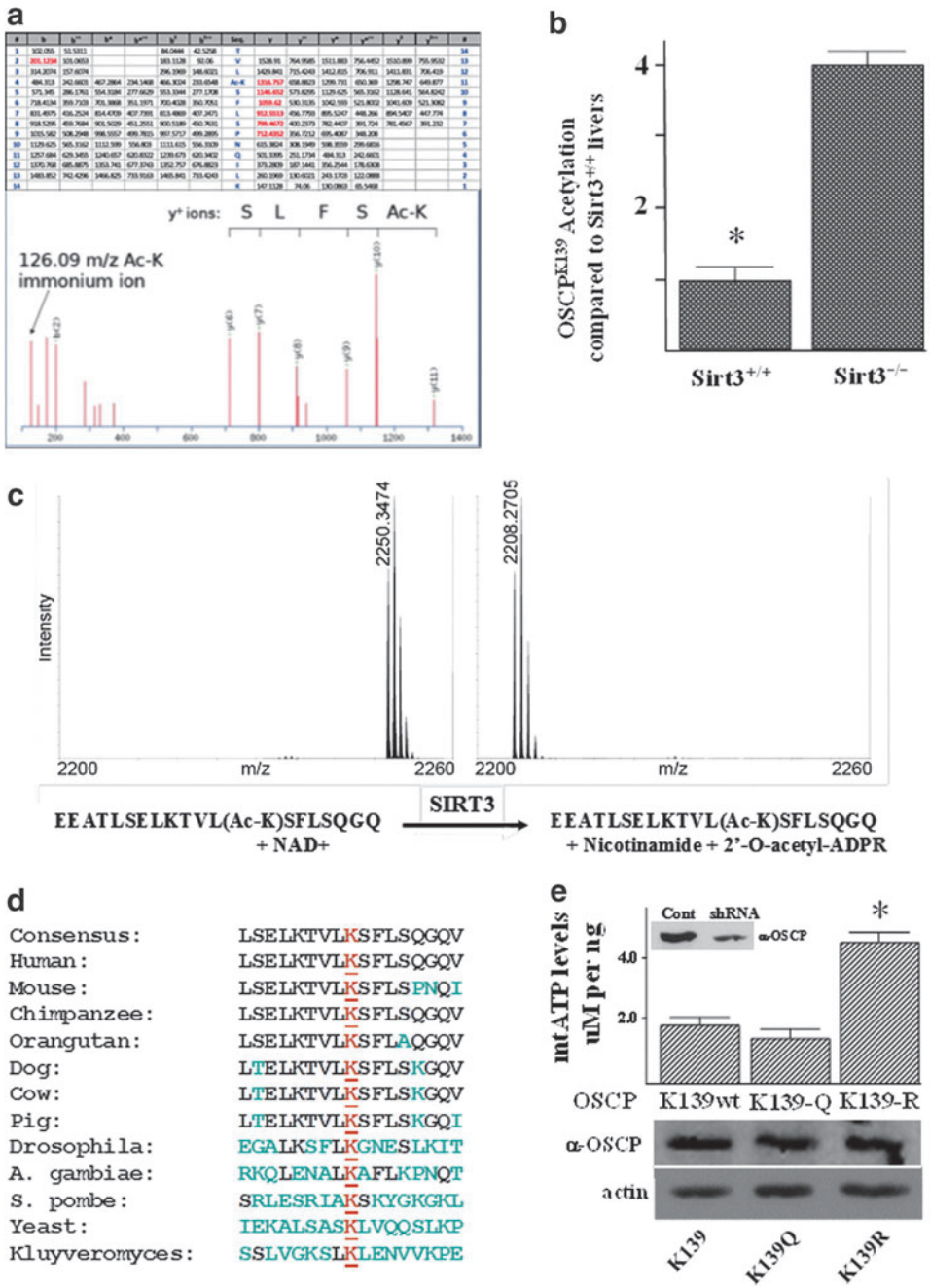

FIG. 3. SIRT3 deacetylates lysine 139. (a) Tandem mass spectrum from OSCP demonstrates acetylated lysine 139 *in vivo*. Liver mitochondria from wild-type and Sirt3$^{-/-}$ mice were resolved by SDS-PAGE followed by in-gel trypsin digestion, separation by nano-scale reverse-phase chromatography on reverse-phase columns, and analysis by OrbiTrap analyzer *via* an electro-spray interface. The spectrum represents the fragmentation of the peptide with a mass of 1628.9501 corresponding to the sequence TVL(AcK)SFLSPNQILK. **(b)** OSCP acetylation in *Sirt3* wild-type and knockout mice. Livers from Sirt3$^{+/+}$ and Sirt3$^{-/-}$ mice were used to isolate mitochondrial extracts that were used to determine the acetylation levels of OSCP amino acid 139. Data are presented as OSCP^{K139} acetylation as compared with *Sirt3*$^{+/+}$ livers. **(c)** *In vitro* deacetylation of synthetic peptides. Synthetic peptide, including acetylated lysine, corresponding to the sequence of ATP synthase subunit OSCP (sequence EEATLSELKTVL(AcK)SFLSQGQ), was measured by MALDI-TOF (left). The predicted m/z for acetylated peptide is 2250.57 and for deacetylated peptide, it is 2208.56 m/z. **(d)** Multiple species contain a potentially reversible acetyl-lysine. The OSCP protein sequence from multiple species was BLASTed based on the reversible acetyl-lysine located at amino acid 139 in humans and mice. A 17-amino-acid motif (LSELKTVLK*SFL-SQGQV) was identified, and this motif is present in multiple species. **(e)** Deacetylated OSCP increases mitochondrial ATP levels. HCT116 cells expressing an OSCP shRNA (Santa Cruz Biotechnology, Inc.; see inset) were infected with lenti-OSCP^{K139}, lenti-OSCP$^{K139\text{-}N}$, or lenti-OSCP$^{K139\text{-}R}$, and ATP levels were determined as described earlier (Fig. 2c legend). Equal expression of these proteins was determined (lower panel) using an anti-OSCP antibody (Santa Cruz Biotechnology, Inc.). Experiments were done in triplicate, and error bars represent one standard deviation. *Indicates $p < 0.05$ by *t*-test.

was incubated with recombinant SIRT3 (BioMol, Inc.) and NAD+, and the reaction was monitored by MALDI-TOF measurement of the peptide mass (Fig. 3c). After incubation of the acetylated synthetic peptide with recombinant SIRT3, all of the peptide was reduced in mass by 42 m/z. A control reaction with nicotinamide (an inhibitor of sirtuins) caused no shift in the signal, nor did a control with NAD+ and no SIRT3 (data not shown). Similar experiments were performed on a related peptide with acetylated threonine instead of a lysine (sequence EEATLSELK(AcT)VLKSFL SQGQ), with no evidence of deacetylation (Supplementary Fig. S3A).

Acetylation status of lysine 139 of OSCP directs ATP levels

OSCP is an old, evolutionarily conserved protein which is present in most species and, as such, if a specific OSCP lysine is an acetylation target in the regulation of enzymatic activity, it seems reasonable that this lysine would be conserved in multiple mammalian and nonmammalian species. A BLAST search demonstrated a conserved 17-amino-acid motif (LSELKTVLK*SFLSQGQV) around the lysine of interest at amino acid position 139 that is present in human, murine, bovine, and yeast species (Fig. 3d). Thus, it seems reasonable to propose that this conserved motif, which has remained roughly intact in multiple species, may be of biological and physiological importance.

It has previously been shown that substitution of a lysine with an asparagine mimics the acetylated lysine state, while substitution with an arginine mimics deacetylation (15, 22, 27). Thus, mutating lysine 139 to arginine would be predicted to mimic a deacetylated lysine, while substitution with an asparagine would be expected to mimic an acetylated lysine (Supplementary Fig. S3B). To determine whether the acetylation status of OSCP may direct, at least in part, some aspect of ATP synthase activity, HCT116 cells were generated that stably express lenti-OSCP^{K139} (HCT116-OSCP^{K139}), lenti-OSCPK$^{139\text{-}R}$ (HCT116-OSCP$^{K139\text{-}R}$), or lenti-OSCPK$^{139\text{-}N}$ (HCT116-OSCP$^{K139\text{-}N}$). Silencing of endogenous *OSCP* expression was accomplished by using shRNA targeting the 3′ untranslated region. These experiments demonstrated that the OSCP$^{K139\text{-}R}$ mutant increased ATP levels (Fig. 3e, upper panel). The levels of exogenously expressed OSCP in these permanent cell lines were roughly equal (Fig. 3e, lower panel). These results suggest that acetylation of OSCP plays a role, at least in part, in regulating ATP synthase activity.

Finally, an examination of the published three-dimensional OSCP structure from the top and the side (Supplementary Fig. S3C, D) shows that lysine 139 is on the matrix-accessible portion of the OSCP protein as well as of the ATP synthase complex. This location is an ideal position in which to interact with other proteins, such as SIRT3. The results of these experiments confirm that OSCP is a SIRT3 deacetylation target *in vitro* and *in vivo*, that OSCP lysine 139 is a direct SIRT3 target, and indirectly suggest that at least one ATP synthase protein targeted by SIRT3 can direct energy production by changes in acetylation.

OSCP lysine 139 acetylation changes physiological conditions thought to activate SIRT3

To begin to determine the physiological significance of OSCP acetylation, as well as to confirm lysine 139 as a legitimate deacetylation target, an anti-acetyl-lysine 139 OSCP antibody was made (Epitomics, Inc.). To validate whether this antibody was specific for acetylated OSCP at lysine 139, HEK 293T cells were transfected with a cytomegalovirus (CMV)-based plasmid expressing a Flag-tagged WT OSCP protein. These cells were maintained in 1 μM trichostatin A and after 48 h, the exogenous OSCP was IPed with an anti-Flag antibody. Equal amounts of IPed OSCP were incubated with purified SIRT3 protein (BioMol, Inc.) with or without NAD+, which is required to induce SIRT3 deacetylation activity. These samples were subsequently separated and incubated with the anti-acetyl-lysine 139 OSCP antibody. These experiments demonstrated that OSCP immunoreactive protein is decreased in the sample containing SIRT3 and NAD+ as compared with the samples incubated without NAD+ (Fig. 4a, lane 2 *vs.* 1). These *in vitro* experiments were repeated with 2 h of preincubation with the 13-amino-acid lysine 139 acetylated peptide (Ac-peptide) that was initially used to make the antibody (Fig. 4a, lanes 5 and 6) or an identical control 13-amino-acid peptide which lacks an acetyl molecule at position 139 (lanes 3 and 4). Incubation with the acetylated peptide, but not with the control, nonacetylated peptide, prevented immunostaining with the anti-OSCP$^{Ac\text{-}K139}$ antibody. These results indicate that this antibody is specific for acetylated lysine 139 and that SIRT3 deacetylates OSCP in an *in vitro*/cell-free experimental model system.

To determine whether OSCP lysine 139 is deacetylated by SIRT3 *in vivo*, OSCP acetylation status was checked under conditions of nutrient stress. Since SIRT3 activity is induced by calorie restriction (CR), it seemed reasonable to determine the acetylation status of OSCP by using the OSCP$^{Ac\text{-}K139}$ antibody. Two additional anti-acetyl-lysine antibodies to MnSOD lysines 68 and 122, which are also SIRT3-dependent reversible acetyl-lysines (2, 27), were used as controls. A decrease in OSCP acetylation was observed using the anti-OSCP$^{Ac\text{-}K139}$ antibody in WT mice on CR as compared with control mice that were fed an ad libitum diet (Fig. 4b). Similar results were observed using the anti-MnSOD$^{Ac\text{-}K68}$ and -MnSOD$^{Ac\text{-}K122}$ antibodies, demonstrating that OSCP and MnSOD are physiological SIRT3 deacetylation targets. Similar results were also obtained when comparing the WT and *Sirt3* knockout mice that were fasted for 36 h (Supplementary Fig. S4).

It has previously been shown that SIRT3 activity is reduced in mice fed a high-fat diet (HFD), and consistent with this idea, WT mice fed an HFD for 2 months exhibited an increase in OSCP acetylation (Fig. 4c), strongly suggesting a decrease in SIRT3 enzymatic activity. Moreover, higher acetylation of OSCP was detected in the skeletal muscle of Sirt3$^{-/-}$ mice, as compared with Sirt3$^{+/+}$ mice (3rd panel, lanes 3,4 *vs.* 1,2 and lanes 7,8 *vs.* 5,6), by using an anti-K139 OSCP antibody, implying that there is a strong correlation between SIRT3 levels and acetylated levels of OSCP. With regard to total levels of OSCP, we could detect some variation in the total protein levels between different mice, but still the difference in the levels of acetylated OSCP between the Sirt3$^{-/-}$ and Sirt3$^{+/+}$ mice was significant regardless of the total levels of OSCP. This seems reasonable, as we could not find any role of SIRT3 in regulating protein levels of OSCP. Finally, it has also been proposed that sirtuin protein activity decreases with increasing age (22, 24). To address this

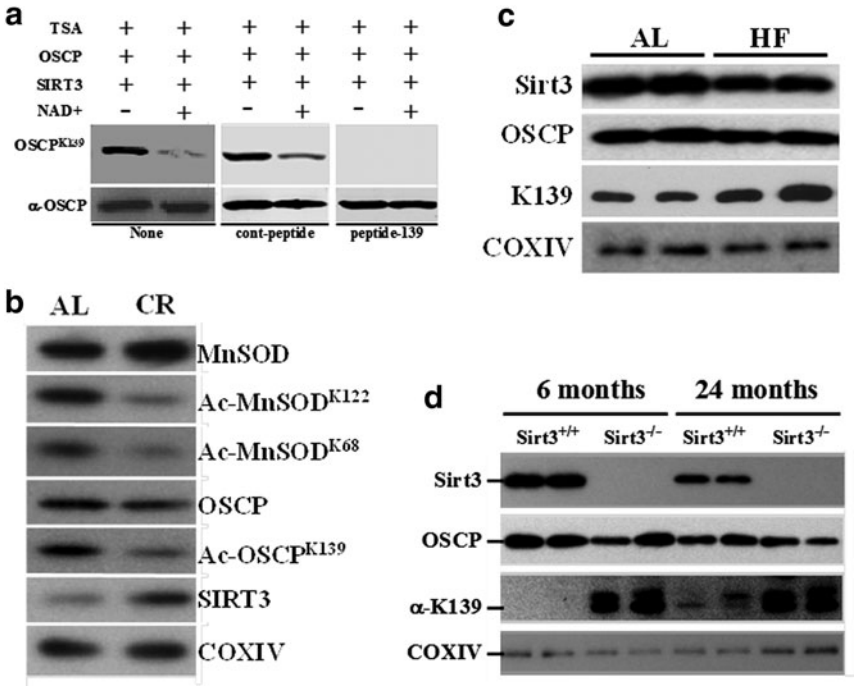

FIG. 4. OSCP contains a physiologically relevant reversible acetyl-lysine under cell stress. (a) Validation of an OSCP lysine 139 anti-acetyl antibody. A Flag-tagged OSCP expression vector was transfected into HEK 293T cells that contained Trichostatin A (TSA) (1 μM) and after 48 h, Flag-OSCP was IPed with an anti-Flag antibody (Sigma, Inc.). The samples were subsequently washed and incubated with purified SIRT3 protein without (lane 1) or with (lane 2) NAD. After 2 h, mixtures were immunoblotted with an anti-Ac-OSCP^{K139} antibody (Epitomics, Inc., - The Rabbit Monoclonal Antibody Company). Identical experiments were done with the 13-amino-acid lysine 139 acetylated peptide (peptide-139) or the control nonacetylated peptide (cont-peptide). **(b)** OSCP contains a CR-dependent, reversible acetyl-lysine. Livers from isogenic, 2-month-old age-matched Sirt3$^{+/+}$ and Sirt3$^{-/-}$ mice that were placed on a CR diet for 12 weeks were harvested and mitochondrial extracts were isolated, separated, and subsequently blotted with antibodies to MnSOD, Ac-MnSOD^{K122}, Ac-MnSOD^{K68}, OSCP, Ac-OSCP^{K139}, SIRT3, and COXIV. **(c)** Wild-type mice were placed on a high-fat ''Western diet'' (TD.88137; Harlan Teklad) as previously shown (30); livers were processed as described earlier, and samples were stained with antibodies to SIRT3, OSCP, Ac-OSCP^{K139}, and COXIV. **(d)** Skeletal muscle from isogenic, 6- and 24-month-old age-matched Sirt3$^{+/+}$ and Sirt3$^{-/-}$ mice were harvested, and mitochondrial extracts were isolated, separated, and blotted with antibodies to SIRT3, OSCP, Ac-OSCP^{K139}, and COXIV.

idea, skeletal muscle samples were taken from WT mice of different ages, and immunoreactive anti-OSCP$^{Ac\text{-}K139}$ protein levels were determined. These experiments demonstrated an increase in OSCP acetylation in WT mice at 24 months (Fig. 4d, lanes 5–6) *versus* those at 6 months of age (lanes 1–2), suggesting that SIRT3 deacetylation of OSCP *in vivo* decreases with increasing age.

Sirt3 $^{-/-}$ *mice exhibit decreased muscle endurance*

The results cited earlier suggest that OSCP acetylation affects, at least in part, the ability of the ATP synthase enzyme to provide energy for the cell through the synthesis of ATP. Since OSCP was strongly detected in skeletal muscle of Sirt3$^{-/-}$ mice, we wanted to determine the role of this phenomenon under energetically demanding conditions. For this purpose, we challenged both WT and *Sirt3*-deficient mice with involuntary physical exercise, testing muscle endurance by running on a treadmill to exhaustion. After acclimatization, mice were run with a protocol using increasing slope and speed until they were unable to run on the treadmill despite electric shocks. Six- and 12-month-old control animals ran an average of 7.1 and 5.3 min longer than the knockout mice: an average of 20.8 min for the controls *versus* 13.7 min for the knockout 6-month-old mice and 17.3 min for the control *versus* 12.0 min for the 12-month-old knockout mice (Fig. 5a).

The difference in running distance was even greater, as the running protocol increased speed with increasing time (Fig. 5b). Sirt3$^{-/-}$ mice covered an average distance of 200.6 and 166.2 meters at 6 and 12 months of age, respectively, whereas control mice ran averages of 358.9 and 277.1 meters (a difference of 44% and 40%, respectively). Finally, the total work performed by control animals was also higher than that of knockouts (Fig. 5c). Control mice used energy equivalent to 1109 J (6 months old) and 847 J (12 months old), whereas the average work of *Sirt3*-deficient mice of the same age was 499 J and 427 J (a difference of 55% and 49%, respectively). In summary, all the parameters obtained from the treadmill running experiment describing muscle endurance were significantly lower for Sirt3$^{-/-}$ mice compared with control mice. Since the *Sirt3* mutant mice used in these experiments were whole body knockout mice, we wanted to exclude the fact that the observed phenotypic differences could reflect additional defects in heart function. Under both basal and

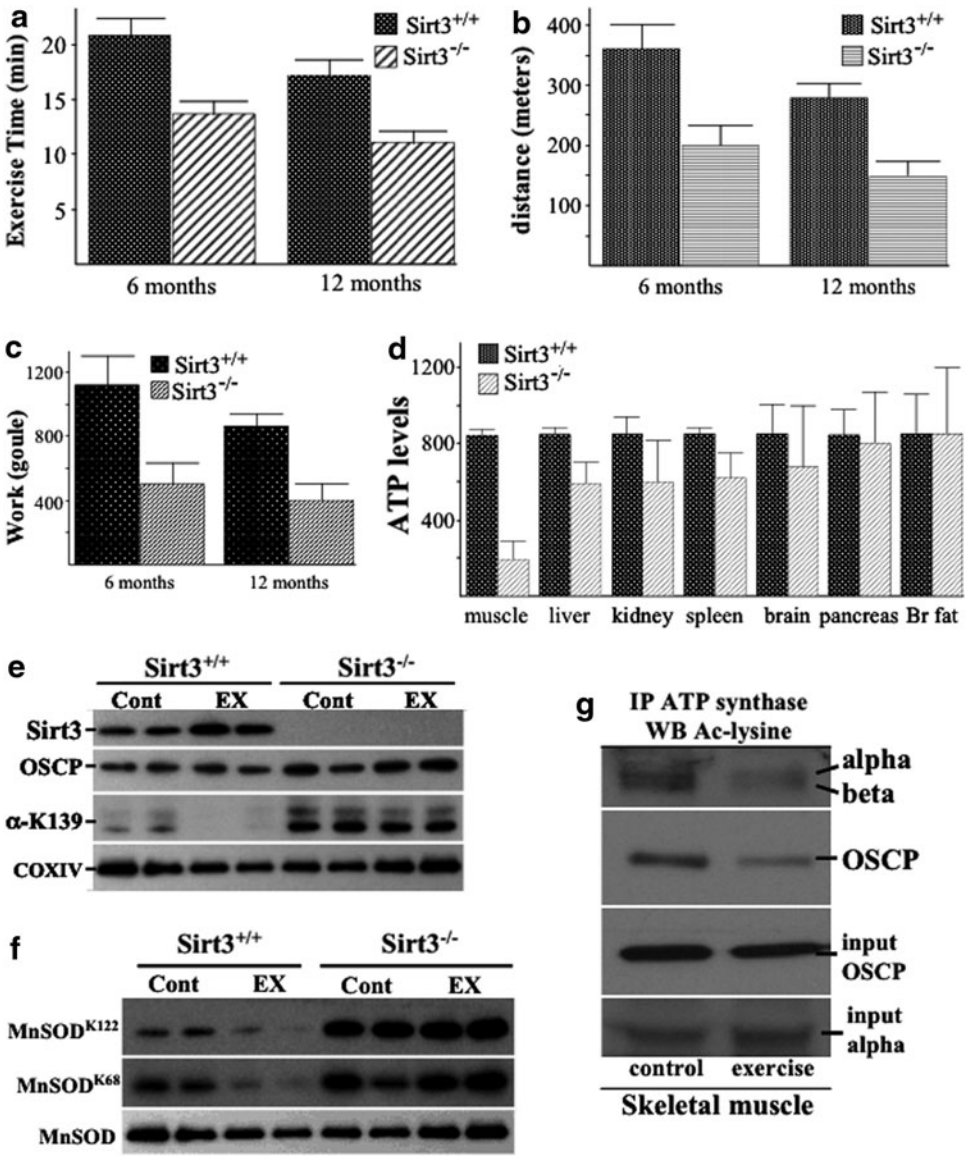

FIG. 5. Sirt3$^{-/-}$ mice exhibit decreased muscle endurance and OSCP is deacetylated in wild-type exercised mice. **(a–c)** After acclimatization, mice were run on a treadmill with increasing speed and slope to exhaustion. Time **(a)**, distance **(b),** and work **(c)** were calculated from the individual performances. Bars represent mean values, and error bars represent standard error. **(d)** Several tissues were harvested from Sirt3$^{+/+}$ and Sirt3$^{-/-}$ mice, and ATP was measured using the ATP determination kit from Molecular Probes. Data are presented as ATP levels measured in *Sirt3*$^{-/-}$ tissue as compared with the *Sirt3*$^{+/+}$ tissue controls. **(e, f)** Skeletal muscle from isogenic Sirt3$^{+/+}$ and Sirt3$^{-/-}$ mice both before exercise (Cont) and immediately after exercise (EX) were harvested and mitochondrial extracts were isolated, separated, and subsequently blotted with antibodies to **(e)** SIRT3, OSCP, Ac-OSCP^{K139}, and COXIV or **(f)** with antibodies to Ac-MnSOD^{K122}, Ac-MnSOD^{K68}, and MnSOD. **(g)** The same samples used earlier were also used to immunoprecipitate the ATP synthase complex (see Fig. 1b), and these samples were immunoblotted with a pan-anti-acetyl antibody (Cell Signaling, Inc.). Representative blots are shown, and experiments were done in triplicate.

stressful conditions, such as beta-adrenergic stimulation where rapid increase in energy demand is needed, no difference in heart or cardiovascular function was found between *Sirt3* WT and mutant mice (Supplementary Fig. S5A, B).

Interestingly, in accordance with the decreased muscle endurance in the Sirt3$^{-/-}$ mice, a significant decrease in ATP levels was observed in skeletal muscle compared with other tissues (Fig. 5d), as well as increased acetylated levels of OSCP, detected by using our anti-OSCP$^{Ac\text{-}K139}$ antibody. More specifically, OSCP was deacetylated in the WT mice upon exercise (Fig. 5e, lanes 3–4 *vs.* 1–2), implying that SIRT3-mediated deacetylation of OSCP enhances ATP synthase enzymatic activity in order to help mice meet the energy demands of the muscle. In contrast, no difference was observed in the mice lacking *Sirt3* (lanes 5–6 *vs.* 7–8), which, as expected, were found to contain hyper-acetylated OSCP. The same pattern was observed when acetylated levels of MnSOD were checked (Fig. 5f), indicating that acetylation of OSCP follows changes in SIRT3 activity and that OSCP is a

specific SIRT3 target in the mitochondrion. In this context, this is a proxy for SIRT3 enzymatic activity and acetylation of the ATP synthase proteins, when skeletal muscle was isolated immediately after the treadmill experiment.

In addition, we assessed the respiratory profile in both C2C12-differentiated myotubes and C2C12-differentiated cells with stable knockdown of *Sirt3* (Supplementary Fig. S6A) using a Seahorse Flux Analyzer. These experiments demonstrated a decrease in basal respiration, coupled respiration, and maximum respiration (Supplementary Fig. S6B, C) in *shSirt3* cells, as compared with controls. Interestingly, we could not see any difference in the levels of uncoupled respiration between control and *shSirt3* myotubes. These results are consistent with our data showing that acetylation of ATP synthase, including OSCP, decreases the function of the complex, resulting in decreased mitochondrial respiration and ATP production.

To exclude the fact that the difference in ATP levels in skeletal muscle was due to the different number of mitochondria in the $Sirt3^{+/+}$ and $Sirt3^{-/-}$ mice, we determined the total number of mitochondria in skeletal muscle, as estimated by real-time quantitative polymerase chain reaction (qPCR) of mitochondrial-encoded genes (NADH dehydrogenase 2, ATP synthase 6, and cytochrome oxidase subunit II) *versus* nuclear-encoded 18S rRNA. These results indicate that the decrease in skeletal muscle ATP levels in the $Sirt3^{-/-}$ mice cannot be attributed to the different number of total mitochondria (Supplementary Fig. S7A). Furthermore, when we compared the shctr-differentiated C2C12 myotubes with the *shSirt3*-differentiated C2C12, no difference in the total number of mitochondria was observed, despite the difference in mitochondrial respiration (Supplementary Fig. S7B), which is in accordance with previously published data (10), thus confirming that SIRT3-mediated deacetylation of ATP synthase regulates its function.

Though these results showed changes in OSCP, we thought it would be informative to perform a more complete *in vivo* investigation of the ATP synthase complex in the skeletal muscle of mice undergoing exercise, as compared with control mice. As such, skeletal muscle from control and exercised mice was harvested, and mitochondrial extracts were prepared, IPed with an anti-ATP synthase antibody, separated, and immunoblotted with a pan-anti-acetyl antibody. These results showed that exercise stress-induced reversible acetyl-lysine(s) are present in ATP synthase α and β complex proteins (Fig. 5g). These results, along with the Western blotting with lysine-specific antibodies to OSCP and MnSOD, suggest that exercise activates SIRT3 to deacetylate ATP synthase complex proteins.

Finally, one outstanding critical question is: Are these lysines also altered or deacetylated in humans undergoing a decrease in nutrient consumption? To address this, samples were compared from patients before and after bariatric surgery, representing an indirect method to investigate changes in human nutritional status. Specifically, percutaneous muscle biopsies of the vastus lateralis muscle from bariatric surgery patients both preoperative and 6 months postoperative were obtained by conchotome with IRB approval. Proteomic results identified several reversible acetyl-lysines in ATP synthase α (two lysines, 167 and 434), β (one lysine, 197), and γ (one lysine, 138), as well as changes in OSCP (lysine 139) and MnSOD (lysines 68 and 122) (Table 3).

Table 3. Acetylation Changes in Human Muscle

		Spectral Count	
Amino acid	*Sequence*	*Pre*	*Post*
ATP synthase subunit alpha			
167	LGNAIDGKGPIGSKT	3	0
434	VAGTMKLELAQYR	4	0
ATP synthase subunit beta			
197	VVDLLAPYAKGGK	4	0
ATP synthase subunit gamma			
138	IKGILYR	4	1
ATP synthase subunit OSCP			
139	TVLKSFLSPNQILK	3	0
ATP synthase subunit MnSOD			
68	NVTEEKYQEALAK	7	2
122	GELLEAKRDFGS	3	0

Samples from human patients before and after bariatric surgery. Pre, preoperative; Post, six months postoperative.

Finally, to determine a commonality between the different lysines that were altered, as shown earlier (Tables 1–3), a bioinformatic analysis was done to identify potential evolutionarily conserved lysines in the ATP synthase complex F_1-protein. ATP synthase α lysines K132, K161, K167, K427, K434, and K539; ATP synthase β lysines K197 and K259; and ATP synthase γ lysines K136, K138, and K154 were found to be conserved in multiple species, including rodent, primate, fish, and *Caenorhabditis elegans* (Supplementary Fig. S8). Thus, the results presented earlier clearly show that the ATP synthase complex contains multiple SIRT3-dependent reversible acetyl-lysines that are deacetylated under conditions of exercise stress as well as potentially other forms of cellular or nutrient stress.

Discussion

One intriguing finding from our and others' previous work was that cells lacking *Sirt3* exhibited altered mitochondrial metabolism, including a significant decrease in mitochondrial ATP levels (1, 11, 26). These results suggest a potential connection between the regulation of ATP production and SIRT3. In this regard, SIRT3 is the primary mitochondrial deacetylase (16), and lysine acetylation has recently emerged as an important, and perhaps critical, post-translational modification that is employed to regulate mitochondrial proteins (3, 22). In addition, large-scale mass spectrometry screening pre- and postcaloric restriction identified reversible acetyl-lysines in 72 mitochondrial proteins from a wide variety of metabolic pathways (23). Based on these results, it seems reasonable to suggest that deacetylation of mitochondrial proteins by SIRT3 may play a role in maintaining and regulating mitochondrial metabolism and function.

A fundamental paradigm in biology is the presence of intracellular sensing proteins that recognize specific cellular conditions and initiate post-translational signaling cascades (6), and these pathways activate the cellular machinery which maintains cellular homeostasis. The most common example of this is the cytoplasmic activation of kinases that phosphorylate a series of downstream targets in response to different environmental conditions, thereby minimizing any potentially permanent cellular detrimental effects (5). The results

presented earlier support this hypothesis, and along with recent findings (11), suggest that mitochondrial sirtuins, including SIRT3, may function as energy requirement sensing proteins whose loss of function may result in a damage-permissive phenotype which leads to aberrant mitochondrial function. These results also suggest, but do not definitively prove, that the mitochondria may contain processes which sense cellular energy states and engage signaling processes to match energy requirements to energy demands, including, but not limited to, regulation of the F_1 portion of the ATP synthase complex.

The active site in the ATP synthase complex is formed by subunits α and β, which are in close proximity to subunits γ and OSCP. These proteins project out of the inner mitochondrial membrane, are matrix accessible, and would seem to be ideal as targets of SIRT3 as well as for directing the enzymatic activity of the ATP synthase complex. Functional experiments were limited to OSCP, which is the location of contact between the peripheral stator stalk and the enzymatically active α and β subunits, but they may serve as a window into the overall function of the ATP synthase complex. Indeed, small alterations in or removal of OSCP can decouple the ATP synthetic activity of the complex from the proton motive force (20). However, it should be mentioned that mitochondrial production of ATP is dictated by several flux control pathways, including adenine-nucleotide translocase, phosphate transporter, and substrate transporters, to name a few. As such, it seems likely that these and other pathways and factors may also be SIRT3 targets or whose function may be indirectly altered by changes in mitochondrial acetylation.

Since OSCP lysine 139 is a part of a beta-helix that interacts with neighboring subunit b, modification of this residue could reasonably alter activity of the ATP synthase complex. Given that x-ray crystallography and intact mass spectrometric measurement of the molecular mass of this subunit have failed to detect ε-acetylation of any lysine in OSCP, either lysine 139 is acetylated in a small proportion of intact ATP synthase molecules at any given time, or else, this lysine is acetylated at times other than when this protein is assembled into a fully formed and functional ATP synthase complex. For example, a modification present in only a small percent of protein complexes could be associated with a secondary function such as uncoupling from the proton motive force or for assembly or disassembly of the complex.

Interestingly, the role of SIRT3 in regulating energy homeostasis by deacetylating ATP synthase is apparent when high energy demand is needed for the cells. In this regard, the *Sirt3* knockout mice do not show an energy-related phenotype under normal conditions; however, these mice exhibit decreased muscle endurance under energetically demanding conditions such as running on a treadmill till exhaustion. This phenomenon is associated with the detection of elevated levels of acetylated OSCP, highlighting the contribution of acetylation-mediated dysfunction of ATP synthase to this phenotype. Interestingly, in a recent study, it was shown that muscle-specific *Sirt3*-deficient mice did not exhibit any difference in the endurance exercise (4). While comparing studies is complex, the experiments presented by these authors differed in several critical ways. For example, the mice used for their exercise experiments were 8-week-old mice whereas the mice used in our experiments were at least 6 months of age, and using younger mice may explain the lack of a measurable phenotype. Moreover, their exercise data were acquired using a 5-degree incline with increasing speed, while our exercise experiments used an initial conditioning step followed by exercise that increased both incline and speed, producing a more intense skeletal muscle cell stress. While our work confirms the marked global hyperacetylation found in both the muscle and liver-specific *Sirt3*-deficient mice, this new SIRT3 exercise-deficient phenotype that is now added to other results showing altered oxidative stress, carcinogenesis, HFD-induced obesity, and insulin resistance (2, 8, 11, 22, 24, 27). Finally, in the last few years, it has been proposed that changes in the acetylome (18) as well as altered Sirtuin biology (17) may alter the physiology of the inflammasome and this raises an intriguing idea: Are the phenotypes observed in mice lacking *Sirt3*, or other Sirtuin knockout mice, at least in some part, due to the aberrant regulation of the inflammasome?

In conclusion, the results presented here clearly demonstrate that the F1 portion of the ATP synthase complex contains multiple SIRT3-dependent reversible acetyl-lysines that are altered in several conditions of metabolic stress, including exercise, CR, fasting, and HFD, in both mice and human samples. While more mechanistic experiments to determine that these other reversible acetyl-lysines in ATP synthase α, β, and γ will have to be confirmed, we would suggest that it seems reasonable to propose that acetylation plays a significant role, at least in part, in directing ATPase activity and that SIRT3 is at least one upstream sensing factor directing the acetylation status of these proteins.

Materials and Methods

Cell lines and purification of protein extracts

MEFs were isolated from E14.5 isogenic $Sirt3^{+/+}$ and $Sirt3^{-/-}$ mice and maintained in a 37°C incubator with 5% CO_2 and 6% oxygen. *Sirt3*$^{+/+}$ or *Sirt3*$^{-/-}$ MEFs (11) were infected at passage 3 with lentiviral vectors expressing either the WT or a DN *Sirt3* gene (1), made by Applied Biological Materials, Inc. Levels of exogenous SIRT3 and OSCP were confirmed by Western blot analysis and PCR analysis (data not shown). The HCT116-OSCP^{K139}, HCT116-OSCP$^{K139\text{-}R}$, and HCT116-OSCP$^{K139\text{-}N}$ cells were constructed by co-infecting cells with a lentiviral system expressing WT OSCP or-site directed mutants where OSCP amino acid 139 was changed to an arginine, which mimics a deacetylated lysine (HCT116-OSCP$^{K139\text{-}R}$) or changed to an asparagine, which mimics an acetylated lysine (HCT116-OSCP$^{K139\text{-}N}$). C2C12 cells were maintained in high-glucose DMEM (Invitrogen) containing 10% fetal bovine serum. For differentiation into myotubes, after confluency, cells were cultured in DMEM with 2% horse serum. Sirt3 shRNA lentiviral constructs were purchased from Thermo Scientific (TRCN0000039329, TRCN0000039331, and TRCN0000039332), and empty pLKO.1 vector was used as a control. Stable Sirt3 knockdown and shRNA control cell lines were generated by viral transduction of C2C12 myoblasts and selection with puromycin.

Mitochondria were solubilized with 1% w/v DDM and diluted to a protein concentration of 5.5 mg/ml. IP was performed using either an antibody already cross-linked to beads or a free antibody. IPed samples were divided into equal samples, separated by SDS-PAGE, and immunoblotted with anti-acetyl (Cell Signaling, Inc.) and anti-OSCP antibodies.

Statistical analysis

All experiments were done at least in triplicate. Data were analyzed by Student's *t*-test, and results were considered significant at $p < 0.05$. Results are presented as mean ± SD.

Mouse tissues

All work with mice was performed at the National Cancer Institute, National Institutes of Health, Bethesda, Maryland, USA, and was approved by the NCI's Animal Care and Use Committee as described in protocol NCI ROB-118 (NCI Radiation Oncology Branch Protocol 118).

Immunoprecipitation, transfections, and immunoblot analysis

IP with anti-OSCP and anti-SIRT3 antibodies and the subsequent western analyses were done as previously described (11). The control for these IP experiments is normalized to rabbit IgG as well as immunoblotting with the control, IPed antibody. Transfections of pCMV-OSCP^{K139} (WT), pCMV-OSCP$^{K139\text{-}R}$, or pCMV-OSCP$^{K139\text{-}N}$ were done as previously described (11). Blots were incubated with horseradish peroxidase-conjugated secondary antibody, analyzed using an ECL protocol (Amersham Biosciences), and visualized in a Fuji Las-3000 dark box (FujiFilm Systems).

Measurement of mitochondrial ATP levels

ATP levels were monitored using a CellTiter-Glo Luminescent Cell Viability Assay as per the manufacturer's instructions (Promega). CellTiter-Glo was added to 10^6 cells and placed on an orbital shaker to induce cell lysis, and samples were read on a chemiluminescence plate reader (Tecam Safire; integration time of 1 s). Data are presented as mean ± SE of luminescence readings from three separate experiments.

Mass spectrometry-based proteomics and analysis

Anti-MnSOD immune complexes from Sirt3$^{+/+}$ and Sirt3$^{-/-}$ mouse liver were separated by SDS-PAGE (4%–20% acrylamide) and stained with colloidal Coomassie Blue G-250 (Invitrogen). Samples were de-stained with 100 μl of 50% acetonitrile and 50 m*M* ammonium bicarbonate. A prominent 22 kDa band present in each gel lane was excised, finely diced, reduced with 45 m*M* DTT for 20 min at 55°C, alkylated with 100 m*M* iodoacetamide for 30 min at room temperature, and digested overnight at 37°C with trypsin. Peptides were extracted with two rounds of 60% acetonitrile and 0.1% trifluoroacetic acid and were then lyophilized to dryness. Digests were resolubilized in 15 μl of 0.1% formic acid and analyzed by liquid chromatography-tandem mass spectrometry (LC-MS/MS). For LC-MS/MS analysis and co-IP methods, see the ''Supplementary Methods'' section.

Immunohistochemical staining

HCT116 cells were grown on cover slips to a confluency of ~50%. Mitotracker (Invitrogen) was prepared in McCoy media at a concentration of 250 n*M* and applied to the cover slips for 30 min. Cells were washed once with McCoy media and once with phosphate-buffered saline (PBS). Cells were fixed with 3.7% formaldehyde for 5 min, permeabilized with 0.1% Triton X-100 for 10 min, and blocked with 10% goat serum for 30 min, all of which were prepared in PBS. Primary antibodies were applied at a dilution of 1:100 in 10% goat serum for 1 h. Secondary antibodies conjugated to either 568 or 488 fluorophore (Invitrogen) were applied at a dilution of 1:1000 for 1 h, and Hoechst 33342 was applied at a concentration of 2 ng/μl for 10 min. Three washes with PBS were performed between each new application. Cells were imaged utilizing a Zeiss laser scanning microscope (510 META) and the Zeiss software package.

Acknowledgments

DG is supported by NCI-1R01CA152601-01, 1R01CA152799-01A1, 1R01CA168292-01A1, and BC093803 from the Department of Defense and a Hirshberg Foundation for Pancreatic Cancer Research Seed Grant Award. C-XD was supported (in part) by the Intramural Research Program of the NIDDK/NIH. TA is supported (in part) by the Intramural Research Program of the NCI and CCR/NIH. JDP is supported by NIA F30AG030839. The authors thank Mike Runswick, MBE, for providing bovine heart ATP synthase. They also thank Kamburapola Jayawardena and Mike Harbour for technical assistance with mass spectrometry. They are grateful to Melissa Stauffer, PhD, of Scientific Editing Solutions, for editorial assistance.

Author Disclosure Statement

No competing financial interests exist.

References

1. Ahn BH, Kim HS, Song S, Lee IH, Liu J, Vassilopoulos A, Deng CX, and Finkel T. A role for the mitochondrial deacetylase Sirt3 in regulating energy homeostasis. *Proc Natl Acad Sci USA* 105: 14447–14452, 2008.
2. Chen Y, Zhang J, Lin Y, Lei Q, Guan KL, Zhao S, and Xiong Y. Tumour suppressor SIRT3 deacetylates and activates manganese superoxide dismutase to scavenge ROS. *EMBO Rep* 12: 534–541, 2011.
3. Choudhary C, Kumar C, Gnad F, Nielsen ML, Rehman M, Walther TC, Olsen JV, and Mann M. Lysine acetylation targets protein complexes and co-regulates major cellular functions. *Science* 325: 834–840, 2009.
4. Fernandez-Marcos PJ, Jeninga EH, Canto C, Harach T, de Boer VC, Andreux P, Moullan N, Pirinen E, Yamamoto H, Houten SM, Schoonjans K, and Auwerx J. Muscle or liver-specific Sirt3 deficiency induces hyperacetylation of mitochondrial proteins without affecting global metabolic homeostasis. *Sci Rep* 2: 425, 2012.
5. Gius D, Botero A, Shah S, and Curry HA. Intracellular oxidation/reduction status in the regulation of transcription factors NF-kappaB and AP-1. *Toxicol Lett* 106: 93–106, 1999.
6. Gius DR, Ezhevsky SA, Becker-Hapak M, Nagahara H, Wei MC, and Dowdy SF. Transduced p16INK4a peptides inhibit hypophosphorylation of the retinoblastoma protein and cell cycle progression prior to activation of Cdk2 complexes in late G1. *Cancer Res* 59: 2577–2580, 1999.
7. Glozak MA, Sengupta N, Zhang X, and Seto E. Acetylation and deacetylation of non-histone proteins. *Gene* 363: 15–23, 2005.
8. Hirschey MD, Shimazu T, Jing E, Grueter CA, Collins AM, Aouizerat B, Stancakova A, Goetzman E, Lam MM, Schwer B, Stevens RD, Muehlbauer MJ, Kakar S, Bass NM, Kuusisto J, Laakso M, Alt FW, Newgard CB, Farese RV, Jr.,

Kahn CR, and Verdin E. SIRT3 deficiency and mitochondrial protein hyperacetylation accelerate the development of the metabolic syndrome. *Mol Cell* 44: 177–190, 2011.
9. Jacobs KM, Pennington JD, Bisht KS, Aykin-Burns N, Kim HS, Mishra M, Sun L, Nguyen P, Ahn BH, Leclerc J, Deng CX, Spitz DR, and Gius D. SIRT3 interacts with the daf-16 homolog FOXO3a in the mitochondria, as well as increases FOXO3a dependent gene expression. *Int J Biol Sci* 4: 291–299, 2008.
10. Jing E, Emanuelli B, Hirschey MD, Boucher J, Lee KY, Lombard D, Verdin EM, and Kahn CR. Sirtuin-3 (Sirt3) regulates skeletal muscle metabolism and insulin signaling via altered mitochondrial oxidation and reactive oxygen species production. *Proc Natl Acad Sci USA* 108: 14608–14613, 2011.
11. Kim HS, Patel K, Muldoon-Jacobs K, Bisht KS, Aykin-Burns N, Pennington JD, van der Meer R, Nguyen P, Savage J, Owens KM, Vassilopoulos A, Ozden O, Park SH, Singh KK, Abdulkadir SA, Spitz DR, Deng CX, and Gius D. SIRT3 is a mitochondria-localized tumor suppressor required for maintenance of mitochondrial integrity and metabolism during stress. *Cancer Cell* 17: 41–52, 2010.
12. Kim HS, Xiao C, Wang RH, Lahusen T, Xu X, Vassilopoulos A, Vazquez-Ortiz G, Jeong WI, Park O, Ki SH, Gao B, and Deng CX. Hepatic-specific disruption of SIRT6 in mice results in fatty liver formation due to enhanced glycolysis and triglyceride synthesis. *Cell Metab* 12: 224–236, 2010.
13. Kim SC, Sprung R, Chen Y, Xu Y, Ball H, Pei J, Cheng T, Kho Y, Xiao H, Xiao L, Grishin NV, White M, Yang XJ, and Zhao Y. Substrate and functional diversity of lysine acetylation revealed by a proteomics survey. *Mol Cell* 23: 607–618, 2006.
14. Kouzarides T. Chromatin modifications and their function. *Cell* 128: 693–705, 2007.
15. Li B, Gogol M, Carey M, Lee D, Seidel C, and Workman JL. Combined action of PHD and chromo domains directs the Rpd3S HDAC to transcribed chromatin. *Science* 316: 1050–1054, 2007.
16. Lombard DB, Alt FW, Cheng HL, Bunkenborg J, Streeper RS, Mostoslavsky R, Kim J, Yancopoulos G, Valenzuela D, Murphy A, Yang Y, Chen Y, Hirschey MD, Bronson RT, Haigis M, Guarente LP, Farese RV, Jr., Weissman S, Verdin E, and Schwer B. Mammalian Sir2 homolog SIRT3 regulates global mitochondrial lysine acetylation. *Mol Cell Biol* 27: 8807–8814, 2007.
17. Lugrin J, Ciarlo E, Santos A, Grandmaison G, dos Santos I, Le Roy D, and Roger T. The sirtuin inhibitor cambinol impairs MAPK signaling, inhibits inflammatory and innate immune responses and protects from septic shock. *Biochim Biophys Acta* 1833: 1498–1510, 2013.
18. Misawa T, Takahama M, Kozaki T, Lee H, Zou J, Saitoh T, and Akira S. Microtubule-driven spatial arrangement of mitochondria promotes activation of the NLRP3 inflammasome. *Nat Immunol* 14: 454–460, 2013.
19. Ozden O, Park SH, Kim HS, Jiang H, Coleman MC, Spitz DR, and Gius D. Acetylation of MnSOD directs enzymatic activity responding to cellular nutrient status or oxidative stress. *Aging (Albany NY)* 3: 102–107, 2011.
20. Rees DM, Leslie AG, and Walker JE. The structure of the membrane extrinsic region of bovine ATP synthase. *Proc Natl Acad Sci USA* 106: 21597–21601, 2009.
21. Robison MM, Ling X, Smid MP, Zarei A, and Wolyn DJ. Antisense expression of mitochondrial ATP synthase subunits OSCP (ATP5) and gamma (ATP3) alters leaf morphology, metabolism and gene expression in Arabidopsis. *Plant Cell Physiol* 50: 1840–1850, 2009.
22. Schwer B, Bunkenborg J, Verdin RO, Andersen JS, and Verdin E. Reversible lysine acetylation controls the activity of the mitochondrial enzyme acetyl-CoA synthetase 2. *Proc Natl Acad Sci USA* 103: 10224–10229, 2006.
23. Schwer B, Eckersdorff M, Li Y, Silva JC, Fermin D, Kurtev MV, Giallourakis C, Comb MJ, Alt FW, and Lombard DB. Calorie restriction alters mitochondrial protein acetylation. *Aging Cell* 8: 604–606, 2009.
24. Schwer B and Verdin E. Conserved metabolic regulatory functions of sirtuins. *Cell Metab* 7: 104–112, 2008.
25. Singh KK. Mitochondria damage checkpoint, aging, and cancer. *Ann NY Acad Sci* 1067: 182–190, 2006.
26. Sundaresan SS, Ramesh P, Sivakumar K, and Ponnuswamy MN. Purification, crystallization and preliminary X-ray analysis of haemoglobin from ostrich (Struthio camelus). *Acta Crystallogr Sect F Struct Biol Cryst Commun* 65: 681–683, 2009.
27. Tao R, Coleman MC, Pennington JD, Ozden O, Park SH, Jiang H, Kim HS, Flynn CR, Hill S, Hayes McDonald W, Olivier AK, Spitz DR, and Gius D. Sirt3-mediated deacetylation of evolutionarily conserved lysine 122 regulates MnSOD activity in response to stress. *Mol Cell* 40: 893–904, 2010.
28. Walker JE and Dickson VK. The peripheral stalk of the mitochondrial ATP synthase. *Biochim Biophys Acta* 1757: 286–296, 2006.
29. Watt IN, Montgomery MG, Runswick MJ, Leslie AG, and Walker JE. Bioenergetic cost of making an adenosine triphosphate molecule in animal mitochondria. *Proc Natl Acad Sci USA* 107: 16823–16827, 2010.
30. Xiao C, Kim HS, Lahusen T, Wang RH, Xu X, Gavrilova O, Jou W, Gius D, and Deng CX. SIRT6 deficiency results in severe hypoglycemia by enhancing both basal and insulin-stimulated glucose uptake in mice. *J Biol Chem* 285: 36776–36784, 2010.

Address correspondence to:
Dr. David Gius
Department of Radiation Oncology
Robert H. Lurie Comprehensive Cancer Center
Feinberg School of Medicine
Northwestern University
Rm 3-119, Lurie Research Bldg.
Chicago, IL 60614

E-mail: david.gius@northwestern.edu

Dr. Chu-Xia Deng
Genetics of Development and Disease Branch
10/9N105, National Institute of Diabetes
and Digestive and Kidney Diseases
National Institutes of Health
10 Center Dr.
Bethesda, MD 20892

E-mail: chuxiad@bldg10.niddk.nih.gov

Date of first submission to ARS Central, May 14, 2013; date of final revised submission, November 6, 2013; date of acceptance, November 18, 2013.

Abbreviations Used

AceCS2 = Acetyl-CoA Synthetase 2
AcK = acetylated Lysine (K)
ADP = adenosine diphosphate
AL = ad libitum
ATP = adenosine triphosphate
C.O = cardiac output
CCR = clinical cancer center
CID = collision-induced dissociation ()
CMV = cytomegalovirus
Cont = control (before exercise)
CR = calorie restriction
DAPI = 4′,6-diamidino-2-phenylindole
DN = deacetylation null
EF = ejection fraction
EX = exercise (after exercise)
GST = glutathione S-transferase
HEK = human embryonic kidney
HFD = high fat diet
HR = heart rate
IHC = immunohistochemistry
IP = immunoprecipitation
IPed = immunoprecipitated
LC-MS/MS = liquid chromatography-tandem mass spectrometry
LvVs = left ventricular volume systole
MEFs = mouse embryonic fibroblasts
MRI = magnetic resonance imaging
NAD = nicotinamide adenine dinucleotide
NCI = National Cancer Institute
NHLBI = National Heart, Lung, and Blood Institute
NIH = National Institutes of Health
OSCP = oligomycin sensitivity-conferring protein
PBS = phosphate buffered saline
PCAF = P300/CBP-associated factor
PCR = polymerase chain reaction
PVDF = polyvinylidene difluoride
SDS-PAGE = sodium dodecyl sulfate polyacrylamide gel electrophoresis
TFE = trifluoroethanol
TSA = trichostatin A
WT = wild-type